## **Inorganic Chemistry**

pubs.acs.org/IC Article

# Facile Addition of B-H and B-B Bonds to an Iron(IV) Nitride Complex

Bao G. Tran, Veronica Carta, Maren Pink, Kenneth G. Caulton,\* and Jeremy M. Smith\*



Cite This: Inorg. Chem. 2022, 61, 19800–19805



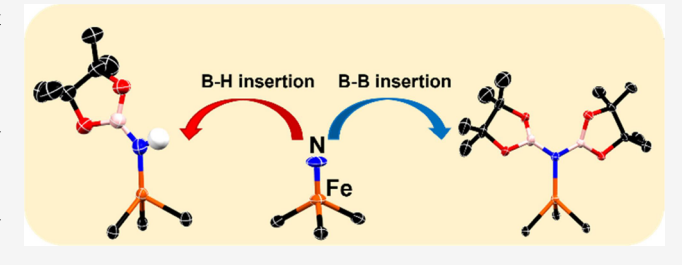
**ACCESS** I

Metrics & More

Article Recommendations

si Supporting Information

**ABSTRACT:** The nitride ligand in the iron(IV) complex  $PhB(^iPr_2Im)_3Fe \equiv N$  reacts with boron hydrides to afford  $PhB(^iPr_2Im)_3FeN(B)H$  (B=9-BBN (1), Bpin (2)) and with (Bpin)<sub>2</sub> to afford  $PhB(^iPr_2Im)_3FeN(Bpin)_2$  (3). The iron(II) borylamido products have all been structurally and spectroscopically characterized, demonstrating facile insertion into B-H and B-B bonds by  $PhB(^iPr_2Im)_3Fe \equiv N$ . Density functional theory (DFT) calculations reveal that the quintet state (S=2) is significantly lower in energy than the singlet (S=0) and triplet (S=1) states for all products. Stoichiometric reaction with (S=1) does not



produce the mono-borylated iron imido species  $PhB({}^{i}Pr_{2}Im)_{3}FeN(Bpin)$ . DFT calculations suggest that this is because  $PhB({}^{i}Pr_{2}Im)_{3}FeN(Bpin)$  is unstable toward disproportionation to the starting Im(IV) nitride and  $PhB({}^{i}Pr_{2}Im)_{3}FeN(Bpin)_{2}$ . Attempts at B-C bond insertion using phenyl- and benzyl-pinacol borane were unsuccessful, which we attribute to unfavorable kinetics.

#### **■ INTRODUCTION**

Transition metal nitrides have garnered interest over the years due to their relevance in dinitrogen fixation, particularly in their conversion to ammonia. While there are multiple reports for the synthesis of nitrides from N<sub>2</sub>, the thermodynamic driving force required to cleave the extremely strong N≡N bond often comes at the expense of subsequent reactivity. Consequently, the selective formation of N-H bonds in N<sub>2</sub>derived nitride complexes has proven to be challenging. For example, it has recently been shown that there is little driving force for N-H bond formation in N2-derived rhenium nitride complexes, where the N-H bond dissociation free energy (BDFE) is less than 50 kcal/mol.<sup>2</sup> Even nitrides that are not generated from N<sub>2</sub> appear to form relatively weak N-H bonds, as demonstrated by an iron(IV) nitride, which only reacts with TEMPO-H (BDFE =  $65.0 \pm 1.3 \text{ kcal/mol}$ ) to generate ammonia.3,4

Given these considerations, we envisioned an alternative strategy for nitride functionalization involving nitride insertion into an H–E bond. Here, we hypothesized that the simultaneous formation of N–H and N–E bonds would provide a greater thermodynamic driving force. For example, hydrogenation of an iridium(III) nitride creates two new N–H bonds in forming the corresponding iridium(I) amido complex.<sup>5</sup> However, although single hydrogen atom transfer to metal nitrides is relatively well studied, examples of nitride insertion into  $\sigma$ -bonds are still uncommon.<sup>3,6–9</sup> With early transition metal complexes, mild electrophilic substrates such as HBpin (HBpin = 4,4,5,5-tetramethyl-1,3,2-dioxaborolane) are remarkably active toward nucleophilic nitrides (Scheme 1).

Scheme 1. Prior Examples of Terminal Nitride Borylation

Received: August 15, 2022 Published: November 28, 2022





For example, Mindiola and co-workers reported Si–H and B–H bond addition to low-coordinate vanadium nitride complexes in 2014. However, it is important to note that the desired B–H insertion reaction is not always observed, as has been demonstrated by Mézailles and co-workers. In this case, the entire  $[\text{Mo}{\equiv}\text{N}]$  unit that is generated from N<sub>2</sub> splitting inserts into the B–H bond of HBpin to provide a borylimido complex, with H on Mo.  $^{11,12}$ 

Over the last decade, we have shown that four-coordinate iron(IV) nitride complexes supported by tris(carbene)borate ligands of varying steric profiles are reactive toward a wide range of substrates, leading to the formation of new N–H and N–C bonds. The diverse reactivity of these complexes can be rationalized according to their frontier orbitals (Figure 1). The electronic structure of *pseudo*-tetrahedral tris-

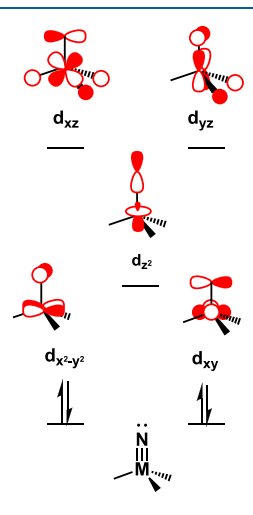


**Figure 1.** Qualitative d-orbital splitting diagram for the tris(carbene)-borate iron(IV) nitride complexes. The LUMO is stabilized by *spd* hybridization.

(carbene)borate iron(IV) nitride complexes reveals that the  $d_{xz}$   $d_{yz}$ , and  $d_z^2$  orbitals are destabilized by bonding with the nitride ligand (z-axis along the Fe–N vector), with the  $d_x^2-d_y^2$  and  $d_{xy}$  essentially nonbonding. Consequentially, the four delectrons are housed in two nonbonding orbitals, allowing access to high valent iron. In addition, density functional theory (DFT) calculations reveal spd hybridization for the  $d_z^2$ -derived LUMO, which lowers its energy by reducing its antibonding character. This allows the LUMO to be an acceptor orbital in two-electron atom transfer reactions. Furthermore, the lone pair on nitrogen, which mixes with the nonbonding Fe  $d_x^2-y^2$  and  $d_{xy}$  orbitals, allows the nitride to act as a nucleophile. As such, our particular iron nitride complexes can be described as being ambiphilic. 17

Recently, we extended these studies to the hydrosilylation of an iron(IV) nitride complex, in which the nitride ligand inserts into Si–H bonds to yield iron(II) amido products. <sup>18</sup> The  $\sigma$ -symmetry LUMO and  $\pi$ -symmetry HOMO of the nitride complex are appropriate for nitride insertion into Si–H bonds, and we reasoned that similar considerations would apply to B–H bond insertion. <sup>15</sup> We further reasoned that the Lewis acidity of the boron atom would provide an additional driving force for the reaction and also lower the reaction barrier (Scheme 2).

In this article, we investigate the reactivity of an iron(IV) nitride complex,  $PhB(^{i}Pr_{2}Im)_{3}Fe \equiv N$ , toward boranes. Herein, we report the first structurally characterized iron(II)

Scheme 2. Facile B-E (E=H, B) Bond Insertion to an Iron Nitride Complex

borylamido complexes. DFT investigation into the energetics of the reactions showed that all likely spin states of products are thermodynamically favorable and suggest that a stepwise pathway is unlikely.

#### ■ RESULTS AND DISCUSSION

Nitride Insertion into B–H and B–B Bonds. The previously reported iron(IV) nitride,  $PhB(^iPr_2Im)_3Fe\equiv N,^{13}$  reacts with equimolar 9-borabicyclo(3.3.1)nonane (9-BBN), which features only  $\sigma$ -donor groups around boron, in room temperature THF to afford the green paramagnetic complex  $PhB(^iPr_2Im)_3FeN(BBN)H$  (1) in 76% isolated yield (Scheme 3). The solid-state molecular structure of 1 has been

Scheme 3. Reaction of Iron Nitride with 9-BBN

determined by single-crystal X-ray diffraction (Figure 2). The Fe–N bond in 1 is longer than that in our previously reported iron silylamido complex, PhB( $^{\text{Mes}}$ Im) $_3$ FeN(H)SiHPh $_2$  (Fe–N = 1.930(4) Å) suggesting less  $\pi$ -donation from nitrogen to the metal center in 1. The N–B bond distance of 1.380(6) Å is slightly shorter than that of Mindiola and co-workers'

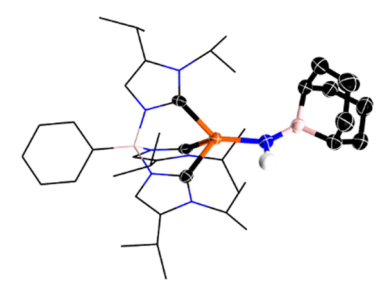


**Figure 2.** Single-crystal X-ray structure of **1**, with thermal ellipsoids shown at 50%, most of the tris(carbene)borate ligand shown as a wire frame, and most hydrogen atoms omitted for clarity. Carbon, hydrogen, nitrogen, boron, and iron atoms are shown in black, white, blue, pink, and orange, respectively.

vanadium borylamido complex (1.396(5) Å). The borylamido moiety in **1** is planar, with the sum of angles equal to  $360^{\circ}$ , suggesting that the nitrogen lone pair is delocalized into the empty p orbital of boron. The Fe-carbene distances (2.080-2.110 Å) are consistent with a high-spin iron(II) tris(carbene)borate complex.

The solid-state structure is maintained in solution. Notably, the  $^1H$  NMR spectrum reveals 13 paramagnetically shifted resonances having relative integrations expected for a three-fold symmetric structure, likely due to rapid rotation around the Fe–N bond. The magnetic moment ( $\mu_{\rm eff}$  = 4.6(2)  $\mu_{\rm B}$ ) is consistent with high spin (S = 2) iron(II).

With the successful addition of 9-BBN to the iron nitride, we hypothesized that a less Lewis acidic borane would react similarly. Thus,  $PhB(^iPr_2Im)_3Fe\equiv N$  reacts with equimolar HBpin at room temperature in THF to yield the brown paramagnetic complex  $PhB(^iPr_2Im)_3FeN(H)(Bpin)$  (2) (Scheme 4) in 83% yield after workup. Like 1, the solid-state structure of 2 was determined by single-crystal X-ray diffraction (Figure 3).

#### Scheme 4. Reaction of Iron Nitride with Pinacolborane

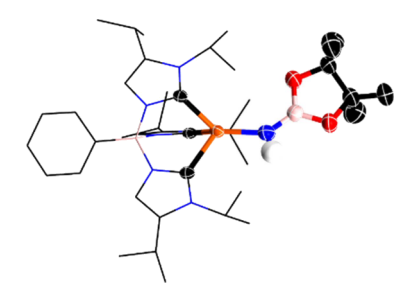
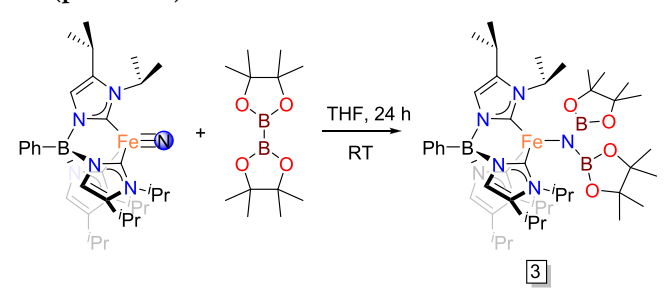


Figure 3. Single-crystal X-ray structure of 1, with thermal ellipsoids shown at 50%, most of the tris(carbene)borate ligand shown as a wire frame, and most hydrogen atoms omitted for clarity. Carbon, hydrogen, nitrogen, oxygen, boron, and iron atoms are shown in black, white, blue, red, pink, and orange, respectively.

The Fe–N bond in **2** of 1.953(6) Å is slightly shorter than that of **1**, and the N–B bond is comparable, at 1.374(10) Å. Complex **2** also exhibits  $C_{3\nu}$  symmetry in solution, as revealed by <sup>1</sup>H NMR spectroscopy. The magnetic moment ( $\mu_{\text{eff}} = 5.1(2) \mu_{\text{B}}$ ) is consistent with high spin (S = 2) iron(II).

We reasoned that two Lewis acidic boron centers would be a stabilizing force, which allows for the lone pair on nitrogen to be delocalized amongst three centers in the putative *bis*-borylamido product. Therefore, we probed the iron(IV) nitride's ability to insert into a B–B bond. The reaction of  $PhB(^iPr_2Im)_3Fe\equiv N$  with equimolar bis(pinacolato)diboron ((Bpin)<sub>2</sub>) in THF at room temperature results in the tan paramagnetic complex  $PhB(^iPr_2Im)_3FeN(Bpin)_2$  (3) in 71% isolated yield (Scheme 5). As with complexes 1 and 2, the  $^1H$ 

### Scheme 5. Reaction of Iron Nitride with Bis(pinacolato)diboron



NMR spectrum is consistent with the complex having threefold symmetry in solution. The magnetic moment ( $\mu_{\rm eff}$  = 4.5(2)  $\mu_{\rm B}$ ) is consistent with high spin (S = 2) iron(II). Moreover, the <sup>57</sup>Fe Mössbauer spectral parameters of 3 ( $\delta$  = 0.64 mm/s;  $\Delta E_{\rm Q}$  = 1.82 mm/s at 80 K) are typical for a high spin (S = 2) iron(II) tris(carbene)borate complex.

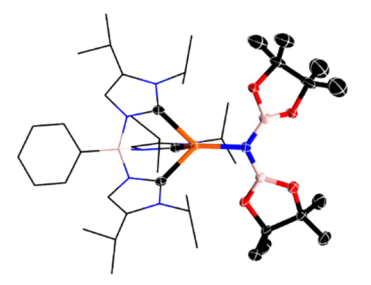


**Figure 4.** Single-crystal X-ray structure of **3**, with thermal ellipsoids shown at 50%, most of the tris(carbene)borate ligand shown as a wire frame, and all hydrogen atoms omitted for clarity. Carbon, nitrogen, oxygen, boron, and iron atoms are shown in black, blue, red, pink, and orange, respectively.

The solid-state structure of 3 confirms the successful insertion of a terminal nitride into the B–B bond (Figure 4). The Fe–N distance (1.999(15) Å) and N–B distances (1.417(2) and 1.409(3) Å) are longer than those of 1 and 2. We attribute these structural differences to the effect of two Lewis acidic boron centers, which reduces the extent of  $\pi$  donation from the nitrogen to the iron center. The greater steric profile of the bis(boryl)amido ligand may also result in a longer Fe–N bond. As with 1 and 2, the nitrogen atom of the borylamido ligand in 3 is planar, with the sum of angles equal to 358.4°. All the other structural metrics are consistent with a high spin iron(II) tris(carbene)borate complex.

Having shown that the nitride ligand can insert into B–H and B–B bonds, we hypothesized that  $PhB(^iPr_2Im)_3Fe \equiv N$  may similarly react with B–C bonds. However, no reaction between  $PhB(^iPr_2Im)_3Fe \equiv N$  and either PhBpin or BnBpin is observed, even at elevated temperatures.

**DFT** Insights into Reaction Thermodynamics and Mechanism. The nitride insertion reactions described above all involve a change in spin state, in which the singlet reactants are converted to quintet products. To obtain insight into the possible influence of spin state changes on the reaction energetics, we used DFT to calculate the thermodynamics for these reactions. For computational expediency, the relative energies for all likely spin states for the iron reactants and products have been calculated with a truncated tris(carbene)-borate ligand in which the isopropyl and borate phenyl groups

are replaced by methyls (complexes 1a-3a). We surveyed a number of different functionals (see SI), and the following results were calculated using B3LYP as functionals and def2-TZVP as the basis set.

## Scheme 6. DFT (B3YLP-def2-TZVP) Calculated $\Delta G^0$ (kcal/mol) for the Formation of Model Compounds 1a, 2a, and 3a

MeB(Me <sub>2</sub> Im) <sub>3</sub> FeN	+	HBpin ——— MeB(Me <sub>2</sub> Im) <sub>3</sub> FeN(H)(Bpin)	( <b>1a</b> )	$\Delta G^0 = -76.4$
MeB(Me <sub>2</sub> Im) <sub>3</sub> FeN	+	9-BBN — MeB(Me <sub>2</sub> Im) <sub>3</sub> FeN(H)(BBN)	(2a)	$\Delta G^0 = -85.3$
MeB(Me <sub>2</sub> Im) <sub>3</sub> FeN	+	(Bpin) <sub>2</sub> — MeB(Me <sub>2</sub> Im) <sub>3</sub> FeN(Bpin) <sub>2</sub>	(3a)	$\Delta G^0 = -107$

These calculations reveal that the formation of complexes 1a-3a by iron nitride insertion into the respective B-H and B-B bonds is thermodynamically favorable (Scheme 6) regardless of spin state, in support of the observed double functionalization of the iron nitride. These calculations also reveal that the formation of 3a is the most thermodynamically favorable, likely due to the formation of two new, stronger N-B bonds upon nitride insertion into the B-B bond. Similarly, the formation of one N-B and one N-H bond likely favors nitride insertion in 1a and 2a.

Since the reaction involves a spin state change, from iron(IV) nitride (S=0) to iron(II) borylamido (S=2), we probed the relative energy of all likely spin states using DFT. As exemplified by the reaction with 9-BBN to afford  $\mathbf{1a}$ , the product quintet state (S=2) is significantly lower in energy than the singlet (S=0) and triplet (S=1) states, which are isoenergetic (Figure 5). This is consistent with experimental

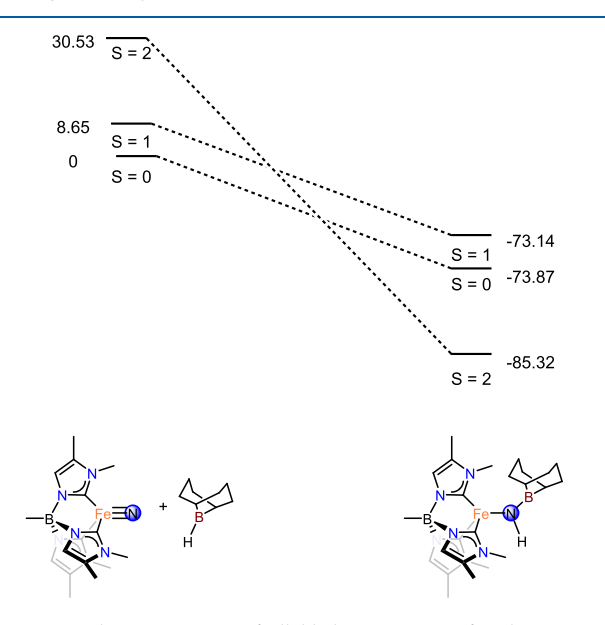


**Figure 5.** Relative energies of all likely spin states for the reaction MeB(Me<sub>2</sub>Im)<sub>3</sub>Fe=N + 9-BBN  $\rightarrow$  MeB(Me<sub>2</sub>Im)<sub>3</sub>Fe-N(BBN)H. Energies are in kcal/mol and are relative to that of MeB-(Me<sub>2</sub>Im)<sub>3</sub>Fe=N (S=0). See Figures S11 and S12 for the relative energies for the other reactions.

observations, where only singlet reactants and a quintet product are observed. The large energy difference between the S=0 and S=2 states for the iron nitride suggests that access to the quintet state prior to N–B bond formation is unlikely. However, the triplet state is energetically accessible and may play a role in the reaction. These results

are consistent with the insertion reaction occurring on either the singlet or triplet surfaces, followed by a rapid spin state change to provide the quintet product. To address this, we determined minimum energy crossing points (MECPs) for all possible spin state changes involving the borylamido product 1a. These calculations show that all the crossing points are downhill from the reactants (-72.5 to -73.6 kcal/mol), see Table S5). The MECP structures reveal long Fe-N bond distances (1.926–1.945 Å). As exemplified by the S = 0/S = 2MECP, the Fe-N bond (1.944 Å) is longer than that of the S = 0 state of 1a (1.917 Å). In addition, the Fe-carbene bond distances are also longer (1.967-2.038 Å) than the S=0 state of 1a (1.901-1.991 Å). These observations are indicative of the transition to a higher spin state. Together with the very negative and similar free energy changes for the crossing points, the MECP structural data suggest that spin state changes occur extremely late in the reaction. Similar results are obtained for the reactions with HBpin and (Bpin)<sub>2</sub>, see Figures S14 and S15.

Although the MECP results suggest that spin state changes are not important to B–H insertion, we also undertook a functional analysis to assess the importance of spin state energies in the formation of 1a (Figures S16–S20). Here, we find that the quintet state (S=2) is greatly lower in energy than the singlet (S=0) and triplet (S=1) states for a set of four different functionals (10-22 kcal/mol lower). The PBE and BLYP functionals erroneously predict the S=0 state to be the lowest in energy. This study shows that the high exothermicity of the reactions is modeled successfully by a number of different functionals (we infer a similar conclusion for the formation of 2a and 3b).

We propose that nitride ligand insertion into the B–H bond of 9-BBN may proceed by one of two pathways: (1) a concerted reaction involving direct nitride insertion into the B–H bond or (2) a stepwise pathway in which formation of a nitride—borane adduct is followed by [1,2]-migration of the hydrogen atom (Scheme 7).

#### Scheme 7. B-E Insertion Pathways

We probed the latter pathway by structurally optimizing the Lewis acid—base adduct of the iron nitride and 9-BBN. For both the singlet and quintet spin states, structural optimization of these adducts resulted in their collapse to the corresponding product structures via migration of the hydrogen atom to the nitrogen, indicating a low barrier to migration. Curiously, structural optimization of the triplet state resulted in a diamond-shaped four-center local minimum structure in which the borane hydrogen atom is also coordinated to iron (Figure 6). While the energy of this unusual species is 33 kcal/mol higher than the triplet state of the product, it is still lower than that of the reagents.

Therefore, we cannot exclude the possibility that such species is formed if the triplet surface is involved in the reaction mechanism.

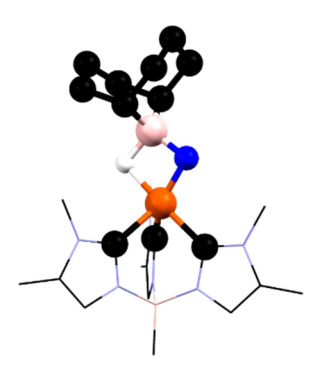


**Figure 6.** Optimized structure of nitride—borane adduct species (S=1) feature a coordinating hydrogen atom on the iron center. Selected bond distances and bond angles: Fe—N 1.697 Å, Fe—H 1.735 Å, N—B 1.467 Å, and B—H 1.410 Å; N—Fe—H 77.5°, Fe—N—B 92.6°, and N—B—H 96.7°.

Since the DFT calculations do not support a stepwise pathway, we therefore favor a concerted mechanism for nitride insertion into the B–H bond. In support of this conclusion, we note that we do not observe the formation of iron nitride—borane Lewis acid/base adduct by <sup>1</sup>H NMR. Similar mechanistic considerations apply to the B–B bond insertion reaction. Additionally, when 0.5 equiv of HBpin and 0.5 equiv of 9-BBN are added to 1 equiv of iron nitride, we only observe the formation of the corresponding borylamido complexes 1 and 2. A stepwise mechanism would be expected to result in the scrambling of the boryl fragments. A control experiment shows that complexes 1 and 2 do not react with each other.

We also used DFT (B3LYP/def2-TZVP) to calculate the energetics of the reaction between the nitride complex and PhBpin. These calculations reveal that the reaction is thermodynamically favorable, with  $\Delta G = -64$  kcal/mol. Similar results are obtained for the reaction with BnBpin. This suggests that the lack of reaction with these substrates is due to an insurmountable kinetic barrier.

It is notable that we do not observe the formation of the monoborylated iron(III) imido species PhB(iPr<sub>2</sub>Im)<sub>3</sub>Fe = N(Bpin) (4) in the reaction of PhB( ${}^{i}$ Pr<sub>2</sub>Im)<sub>3</sub>Fe $\equiv$ N with (Bpin)<sub>2</sub>. Efforts to access this complex by reaction with substoichiometric (Bpin)<sub>2</sub> results only in the formation of 3, along with unreacted nitride complex. In order to explain this absence, we once again turned to DFT for insight. We reasoned that if 4 is formed in the reaction, the thermodynamically favorable disproportionation of 4 to the starting iron(IV) nitride and 3 would account for our experimental observations (Scheme 8). Indeed, the DFT calculated energy for the disproportionation of the truncated complex MeB-(Me<sub>2</sub>Im)<sub>3</sub>FeN(Bpin) is thermodynamically favorable, regardless of spin state. In particular, the disproportionation of the sextet (S = 5/2) of MeB(Me<sub>2</sub>Im)<sub>3</sub>FeN(Bpin) to the singlet (S = 5/2)= 0) MeB(Me<sub>2</sub>Im)<sub>3</sub>Fe $\equiv$ N and quintet (S = 2) of MeB-

#### Scheme 8. Disproportionation of 4 into 3

 $(Me_2Im)_3FeN(Bpin)_2$  is thermodynamically downhill by 36 kcal/mol. This suggests that if complex 4 is ever formed, it undergoes disproportionation with a small energy barrier.

#### SUMMARY AND CONCLUSIONS

The combined synthetic experiments showed facile borylation of an iron(IV) nitride complex. Addition of B-H and B-B bonds to the iron nitride complex was demonstrated via the characterization of complexes 1, 2, and 3. Based on the results for a model system, DFT does not support the formation of nitride and borane acid-base products, suggesting that the stepwise pathway is unlikely. These calculations also reveal that the product quintet (S = 2) states are the most thermodynamically favorable in all cases but do not exclude the involvement of the singlet (S = 0) and triplet (S = 1) states in the reaction mechanism, albeit at a late stage. A disproportionation reaction is proposed to explain the absence of monoborylated iron(III) imido species, which is supported by DFT. Despite successful additions of B-H and B-B bonds to the terminal nitride, B-C bond insertion is unsuccessful, likely due to a kinetic barrier. Our results pave the way toward facile access to coordinated borylamido ligands, featuring Lewis acidic boron centers.

#### ASSOCIATED CONTENT

#### **Supporting Information**

The Supporting Information is available free of charge at https://pubs.acs.org/doi/10.1021/acs.inorgchem.2c02931.

General considerations, preparation of complexes, additional tables with crystallographic parameters; <sup>1</sup>H NMR and mass spectroscopy spectra of complexes; and computational details (PDF)

DFT optimized coordinates (XYZ)

#### **Accession Codes**

CCDC 2194393–2194395 contain the supplementary crystallographic data for this paper. These data can be obtained free of charge via <a href="www.ccdc.cam.ac.uk/data\_request/cif">www.ccdc.cam.ac.uk/data\_request/cif</a>, or by emailing <a href="data\_request@ccdc.cam.ac.uk">data\_request/cif</a>, or by contacting The Cambridge Crystallographic Data Centre, 12 Union Road, Cambridge CB2 1EZ, UK; fax: +44 1223 336033.

CCDC 2194393–2194395 contain the supplementary crystallographic date for this paper. These data can be obtained free of charge via <a href="www.ccdc.cam.ac.uk/data\_request/cif">www.ccdc.cam.ac.uk/data\_request/cif</a> or by emailing <a href="data\_request@ccdc.cam.ac.uk">data\_request@ccdc.cam.ac.uk</a>, or by contacting The Cambridge Crystallographic Data Centre, 21 Union Road, Cambridge CB2 1EZ, UK; fax: +441223 336033.

#### AUTHOR INFORMATION

#### **Corresponding Authors**

Kenneth G. Caulton — Department of Chemistry, Indiana University, Bloomington, Indiana 47405, United States; orcid.org/0000-0003-3599-1038; Email: caulton@indiana.edu

Jeremy M. Smith — Department of Chemistry, Indiana University, Bloomington, Indiana 47405, United States; orcid.org/0000-0002-3206-4725; Email: smith962@indiana.edu

#### Authors

Bao G. Tran – Department of Chemistry, Indiana University, Bloomington, Indiana 47405, United States **Inorganic Chemistry** Article pubs.acs.org/IC

Veronica Carta - Department of Chemistry, Indiana University, Bloomington, Indiana 47405, United States Maren Pink - Department of Chemistry, Indiana University, Bloomington, Indiana 47405, United States; oorcid.org/ 0000-0001-9049-4574

Complete contact information is available at: https://pubs.acs.org/10.1021/acs.inorgchem.2c02931

#### Notes

The authors declare no competing financial interest.

#### ACKNOWLEDGMENTS

This work was supported by the National Science Foundation, Chemical Synthesis Program (SYN), by grants CHE-1955887 to K.G.C. and CHE-1900020 to J.M.S. Support for the acquisition of the Bruker Venture D8 diffractometer through the Major Scientific Research Equipment Fund from the President of Indiana University and the Office of the Vice President for Research is gratefully acknowledged. We thank Dr. Alyssa Cabelof for helpful guidance and insight on DFT.

#### REFERENCES

- (1) Forrest, S. J. K.; Schluschaß, B.; Yuzik-Klimova, E. Y.; Schneider, S. Nitrogen fixation via splitting into nitrido complexes. Chem. Rev. 2021, 121, 6522-6587.
- (2) Connor, G. P.; Delony, D.; Weber, J. E.; Mercado, B. Q.; Curley, J. B.; Schneider, S.; Mayer, J. M.; Holland, P. L. Facile conversion of ammonia to a nitride in a rhenium system that cleaves dinitrogen. Chem. Sci. 2022, 13, 4010-4018.
- (3) Scepaniak, J. J.; Young, J. A.; Bontchev, R. P.; Smith, J. M. Formation of ammonia from an iron nitrido complex. Angew. Chem., Int. Ed. 2009, 48, 3158-3160.
- (4) Agarwal, R. G.; Coste, S. C.; Groff, B. D.; Heuer, A. M.; Noh, H.; Parada, G. A.; Wise, C. F.; Nichols, E. M.; Warren, J. J.; Mayer, J. M. Free energies of proton-coupled electron transfer reagents and their applications. Chem. Rev. 2022, 122, 1-49.
- (5) Schöffel, J.; Rogachev, A. Y.; DeBeer George, S.; Burger, P. Isolation and hydrogenation of a complex with a terminal iridiumnitrido bond. Angew. Chem., Int. Ed. 2009, 48, 4734-4738.
- (6) Wang, D.; Loose, F.; Chirik, P. J.; Knowles, R. R. N-H bond formation in a manganese(V) nitride yields ammonia by light-driven proton-coupled electron transfer. J. Am. Chem. Soc. 2019, 141, 4795-
- (7) Scheibel, M. G.; Abbenseth, J.; Kinauer, M.; Heinemann, F. W.; Würtele, C.; de Bruin, B.; Schneider, S. Homolytic N-H activation of ammonia: Hydrogen transfer of parent iridium ammine, amide, imide, and nitride species. Inorg. Chem. 2015, 54, 9290-9302.
- (8) Bruch, Q. J.; Connor, G. P.; Chen, C.-H.; Holland, P. L.; Mayer, J. M.; Hasanayn, F.; Miller, A. J. M. Dinitrogen reduction to ammonium at rhenium utilizing light and proton-coupled electron transfer. J. Am. Chem. Soc. 2019, 141, 20198-20208.
- (9) (a) Crevier, T. J.; Bennett, B. K.; Soper, J. D.; Bowman, J. A.; Dehestani, A.; Hrovat, D. A.; Lovell, S.; Kaminsky, W.; Mayer, J. M. C-N bond formation on addition of aryl carbanions to the electrophilic nitrido ligand in TpOs(N)Cl2. J. Am. Chem. Soc. 2001, 123, 1059-1071. (b) Crevier, T. J.; Mayer, J. M. Insertion of an osmium nitride into boron-carbon bonds. Angew. Chem. Int. Ed. **1998**, 37, 1891–1893.
- (10) Thompson, R.; Tran, B. L.; Ghosh, S.; Chen, C.-H.; Pink, M.; Gao, X.; Carroll, P. J.; Baik, M.-H.; Mindiola, D. J. Addition of Si-H and B-H bonds and redox reactivity involving low-coordinate nitrido-vanadium complexes. Inorg. Chem. 2015, 54, 3068-3077.
- (11) Espada, M. F.; Bennaamane, S.; Liao, Q.; Saffon-Merceron, N.; Massou, S.; Clot, E.; Nebra, N.; Fustier-Boutignon, M.; Mézailles, N. Room-temperature functionalization of N<sub>2</sub> to borylamine at a

- molybdenum complex. Angew. Chem., Int. Ed. 2018, 57, 12865-
- (12) Bennaamane, S.; Espada, M. F.; Mulas, A.; Personeni, T.; Saffon-Merceron, N.; Fustier-Boutignon, M.; Bucher, C.; Mézailles, N. Catalytic reduction of N<sub>2</sub> to borylamine at a molybdenum complex. Angew. Chem., Int. Ed. 2021, 60, 20210-20214.
- (13) Martinez, J. L.; Lin, H.-J.; Lee, W.-T.; Pink, M.; Chen, C.-H.; Gao, X.; Dickie, D. A.; Smith, J. M. Cyanide ligand assembly by carbon atom transfer to an iron nitride. J. Am. Chem. Soc. 2017, 139, 14037-14040.
- (14) Muñoz, S. B., III; Lee, W.-T.; Dickie, D. A.; Scepaniak, J. J.; Subedi, D.; Pink, M.; Johnson, M. D.; Smith, J. M. Styrene aziridination by iron(IV) nitrides. Angew. Chem., Int. Ed. 2015, 54, 10600-10603.
- (15) Scepaniak, J. J.; Bontchev, R. P.; Johnson, D. L.; Smith, J. M. Snapshots of complete nitrogen atom transfer from an iron(iv) nitrido complex. Angew. Chem., Int. Ed. 2011, 50, 6630-6633.
- (16) Lee, W.-T.; Juarez, R. A.; Scepaniak, J. J.; Muñoz, S. B.; Dickie, D. A.; Wang, H.; Smith, J. M. Reaction of an iron(IV) nitrido complex with cyclohexadienes: Cycloaddition and hydrogen-atom abstraction. Inorg. Chem. 2014, 53, 8425-8430.
- (17) Scepaniak, J. J.; Fulton, M. D.; Bontchev, R. P.; Duesler, E. N.; Kirk, M. L.; Smith, J. M. Structural and spectroscopic characterization of an electrophilic iron nitrido complex. J. Am. Chem. Soc. 2008, 130, 10515-10517.
- (18) Valdez-Moreira, J. A.; Millikan, S. P.; Gao, X.; Carta, V.; Chen, C.-H.; Smith, J. M. Hydrosilylation of an iron(IV) nitride complex. Inorg. Chem. 2020, 59, 579-583.
- (19) Shaik, S.; Danovich, D.; Fiedler, A.; Schröder, D.; Schwarz, H. Two-state reactivity in organometallic gas-phase ion chemistry. Helv. Chim. Acta 1995, 78, 1393-1407.
- (20) Sun, Y.; Tang, H.; Chen, K.; Hu, L.; Yao, J.; Shaik, S.; Chen, H. Two-state reactivity in low-valent iron-mediated C-H activation and the implications for other first-row transition metals. J. Am. Chem. Soc. **2016**, 138, 3715-3730.

### **Ⅲ** Recommended by ACS

#### Hydroboration of the (C<sub>5</sub>Me<sub>5</sub>)Fe(1,2-Ph<sub>2</sub>PC<sub>6</sub>H<sub>4</sub>) System To **Derive Hydridoborate and Hydridosilicate Complexes**

Rui Sun, Wenguang Wang, et al.

AUGUST 24 2022 **ORGANOMETALLICS** 

READ 2

Mechanistic Studies of Alkyne Hydroboration by a Well-**Defined Iron Pincer Complex: Direct Comparison of Metal-Hydride and Metal-Boryl Reactivity** 

Ana L. Narro, Zachary J. Tonzetich, et al.

JUNE 29, 2022

INORGANIC CHEMISTRY

READ **C** 

#### Iron Dihydride Complex Stabilized by an All-Phosphorus-**Based Pincer Ligand and Carbon Monoxide**

Bedraj Pandey, Hairong Guan, et al.

JULY 11, 2022

INORGANIC CHEMISTRY

READ **C** 

#### Coordination Chemistry of (Triphos)Fe(0) Ethylene Complexes and Their Application to CO<sub>2</sub> Valorization

Tristan T. Adamson, Wesley H. Bernskoetter, et al.

OCTOBER 19, 2022

ORGANOMETALLICS

READ **C** 

Get More Suggestions >